SISSA 79/2005/EP

Neutrino oscillations: Current status and prospects*

Thomas Schwetz

Scuola Internazionale Superiore di Studi Avanzati (SISSA)
Via Beirut 2–4, I–34014 Trieste, Italy

Abstract

I summarize the status of neutrino oscillations from world neutrino oscillation data with date of October 2005. The results of a global analysis within the three-flavour framework are presented. Furthermore, a prospect on where we could stand in neutrino oscillations in ten years from now is given, based on a simulation of upcoming long-baseline accelerator and reactor experiments.

1 Introduction

In the last ten years or so we have witnessed huge progress in neutrino oscillation physics. The outstanding experimental results lead to quite a clear overall picture of the neutrino sector. We know that there are two mass-squared differences separated roughly by a factor of 30, and in the lepton mixing matrix there are two large mixing angles, and one mixing angle which has to be small. In the first part of this talk I review the present status of neutrino oscillations by reporting the results of a global analysis of latest world neutrino oscillation data from solar, atmospheric, reactor and accelerator experiments. This analysis is performed in the three-flavour framework and represents an update of the work published in Refs. [1, 2].

The recent developments in neutrino oscillations triggered a lot of activity in the community, and many new neutrino oscillation experiments are under construction, or under active investigation, to address important open questions, such as the value of the small mixing angle θ_{13}, leptonic CP violation and the type of the neutrino mass hierarchy. In the second part of the talk I try to give an outlook, where we could stand in about ten years from now. These results are based on a simulation of up-coming long-baseline accelerator and reactor experiments, which are expected to deliver physics results within the anticipated time scale [3, 4].

*Talk given at the XXIX International Conference of Theoretical Physics, "Matter To The Deepest: Recent Developments In Physics of Fundamental Interactions", 8–14 September 2005, Ustron, Poland.

parameter	bf$\pm 1\sigma$	1σ acc.	3σ range
Δm^2_{21} $[10^{-5}\mathrm{eV}^2]$	7.9 ± 0.3	4%	$7.1 - 8.9$
$\lvert\Delta m^2_{31}\rvert$ $[10^{-3}\mathrm{eV}^2]$	$2.2^{+0.37}_{-0.27}$	14%	$1.4 - 3.3$
$\sin^2\theta_{12}$	$0.31^{+0.02}_{-0.03}$	9%	$0.24 - 0.40$
$\sin^2\theta_{23}$	$0.50^{+0.06}_{-0.05}$	11%	$0.34 - 0.68$
$\sin^2\theta_{13}$	$-$	$-$	≤ 0.046

Table 1: Best fit values (bf), 1σ errors, relative accuracies at 1σ, and 3σ allowed ranges of three-flavour neutrino oscillation parameters from a combined analysis of global data, updated from Ref. [2].

Three-flavour neutrino oscillations are described in general by the two independent mass-squared differences Δm^2_{21}, Δm^2_{31}, three mixing angles $\theta_{12}, \theta_{23}, \theta_{13}$, and one complex phase δ_{CP}. Throughout this work I will use the standard parameterization for the PMNS lepton mixing matrix

$$U = \begin{pmatrix} 1 & 0 & 0 \\ 0 & c_{23} & s_{23} \\ 0 & -s_{23} & c_{23} \end{pmatrix} \begin{pmatrix} c_3 & 0 & e^{-i\delta_{\mathrm{CP}}} s_{13} \\ 0 & 1 & 0 \\ -e^{i\delta_{\mathrm{CP}}} s_{13} & 0 & c_{13} \end{pmatrix} \begin{pmatrix} c_{12} & s_{12} & 0 \\ -s_{12} & c_{12} & 0 \\ 0 & 0 & 1 \end{pmatrix} \qquad (1)$$

with the abbreviations $s_{jk} \equiv \sin\theta_{jk}$, $c_{jk} \equiv \cos\theta_{jk}$. The type of the neutrino mass hierarchy is determined by the sign of Δm^2_{31}: $\Delta m^2_{31} > 0$ corresponds to the normal hierarchy and $\Delta m^2_{31} < 0$ to the inverted one.

2 Present status of three-flavour neutrino oscillations

In Tab. 1 I summarize the present status of three-flavour neutrino oscillation parameters. The numbers are obtained from a global analysis of current oscillation data from solar [5–7], atmospheric [8], reactor [9, 10], and accelerator [11] data. Details of the analysis can be found in Ref. [2] and references therein. In the following I give some brief comments on the determination of the 'atmospheric' and the 'solar' parameters, and on the bound on θ_{13}.

The 'atmospheric parameters'. In Fig. 1 I show the allowed regions for θ_{23} and Δm^2_{31} from separate analyses of Super-K atmospheric neutrino data [8], and data from the K2K long-baseline experiment [11]. The latter probes the ν_μ disappearance oscillation channel in the same region of Δm^2 as explored by atmospheric neutrinos. The neutrino beam is produced at the KEK proton synchrotron, and originally consists of 98% muon neutrinos with a mean energy of 1.3 GeV. The ν_μ content of the beam is observed at the Super-K detector at a distance of 250 km, where 107 events have been detected, whereas 151^{+12}_{-10} have been expected for no oscillations. Fig. 1 illustrates that the neutrino mass-squared difference indicated by the ν_μ disappearance observed in K2K is in perfect agreement with atmospheric neutrino oscillations. Hence, K2K data provide the first confirmation of oscillations with Δm^2_{31} from a man-made neutrino source. K2K gives a rather weak constraint on the mixing angle due to low statistics in the current data sample, and the constraints on $\sin^2\theta_{23}$ of Tab. 1 are dominated by atmospheric data. Both data sets give a best fit point of $\theta_{23} = \pi/4$, *i.e.* maximal mixing.

In our analysis of atmospheric neutrino data we neglect the small contribution of os-

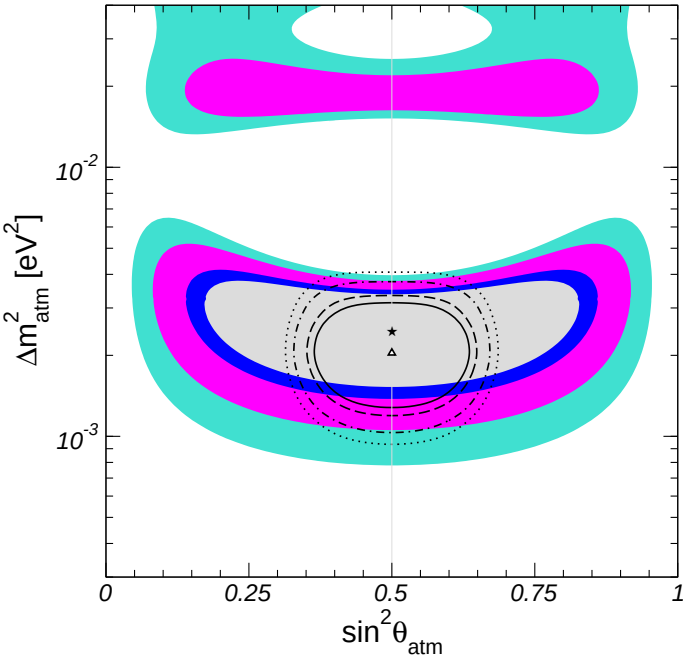

Figure 1: Allowed regions for $\sin^2\theta_{23}$ and Δm^2_{31} at 90%, 95%, 99%, and 3σ C.L. for atmospheric neutrino data (contour lines) and the K2K long-baseline experiment (coloured regions).

cillations with Δm^2_{21}. Taking into account this sub-leading effect, in Refs. [12, 13] a small deviation from maximal mixing was found, due to an excess of sub-GeV e-like events. This indication currently is not statistically significant (about 0.5σ), and so-far it has not been confirmed by a three-flavour analysis of the Super-K collaboration [14].

The 'solar parameters'. In Fig. 2 the allowed regions for θ_{12} and Δm^2_{21} from analyses of solar and KamLAND data are shown. Details of our solar neutrino analysis can be found in Ref. [1] and references therein. We use the same data as in Ref. [2] from the Homestake, SAGE, GNO, and Super-K experiments [5], and the SNO day-night spectra from the pure D_2O phase [6], but the CC, NC, and ES rates from the SNO salt-phase are updated according to the latest 2005 data [7]. For the KamLAND analysis we are using the data equally binned in $1/E_{\rm pr}$ ($E_{\rm pr}$ is the prompt energy deposited by the positron), and we include earth matter effects and flux uncertainties following Ref. [15] (see the appendix of Ref. [2] for further details). We observe from the figure a beautiful agreement of solar and KamLAND data. Moreover, the complementarity of the two data sets allows a rather precise determination of the oscillation parameters: The evidence of spectral distortion in KamLAND data provides a strong constraint on Δm^2_{21}, and leads to the remarkable precision of 4% at 1σ (compare Tab. 1). As visible in the right panel of Fig. 2, alternative solutions around $\Delta m^2_{21} \sim 2 \times 10^{-4}$ eV^2 ($\sim 1.4 \times 10^{-5}$ eV^2), which are still present in the KamLAND-only analysis at 99% C.L., are ruled out from the combined KamLAND+solar analysis at about 4σ (5σ). In contrast to Δm^2_{21}, the determination of the mixing angle is dominated by solar data. Especially recent results from the SNO experiment provide a strong upper bound on $\sin^2\theta_{12}$, excluding maximal mixing at more than 5σ.

The bound on θ_{13}. For the third mixing angle currently only an upper bound exists. This bound is dominated by the CHOOZ reactor experiment [10], in combination with the Δm^2_{31}-determination from atmospheric and K2K experiments. However, recent improved data of

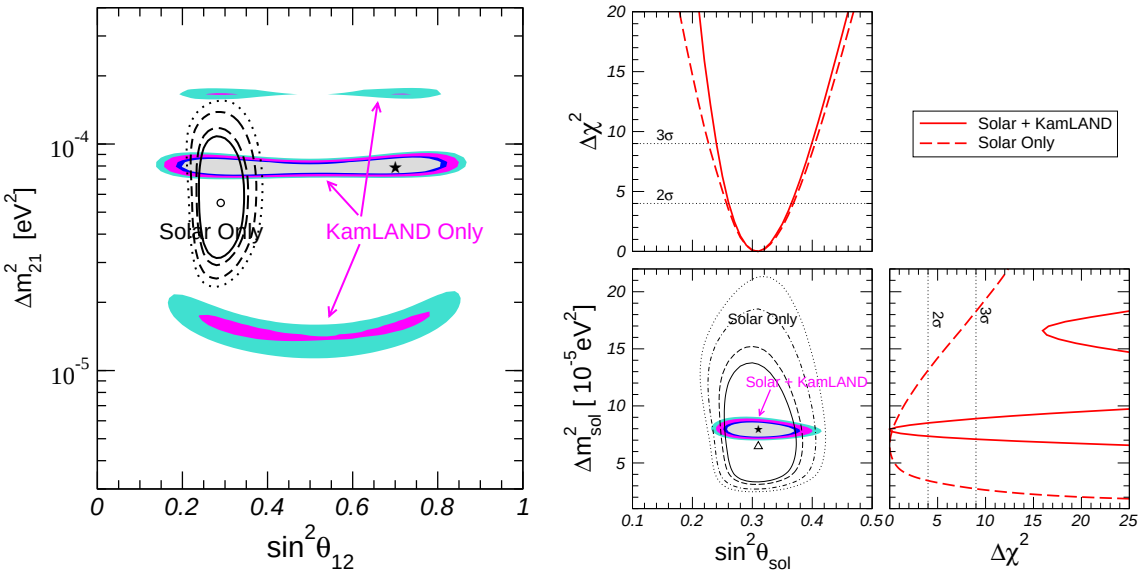

Figure 2: Left: Allowed regions for $\sin^2\theta_{12}$ and Δm^2_{21} at 90%, 95%, 99%, and 3σ C.L. for solar neutrino data (contour lines) and the KamLAND reactor experiment (coloured regions). Right: Combined solar+KamLAND analysis. Also shown is the allowed region from solar data only (contour lines).

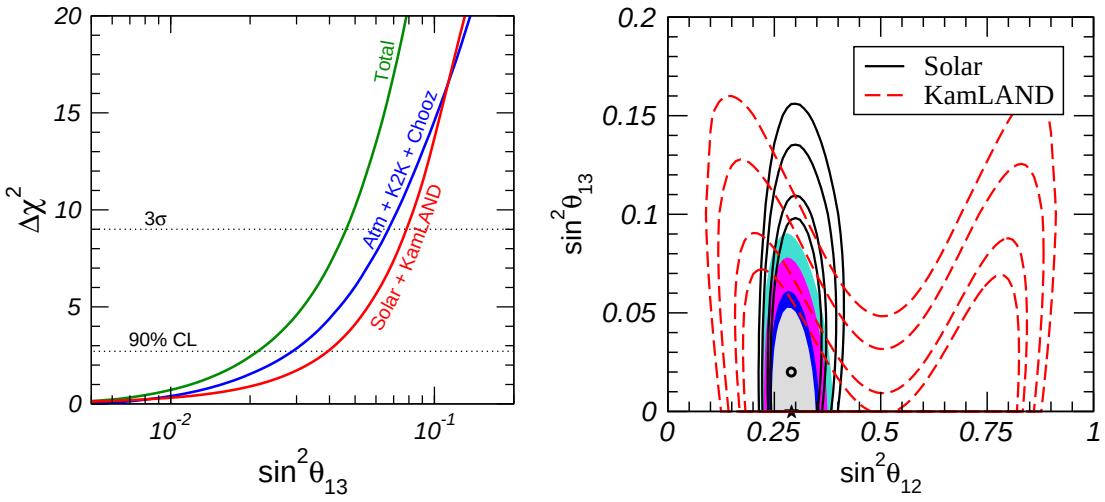

Figure 3: Left: $\Delta\chi^2$ as a function of $\sin^2\theta_{13}$ for solar+KamLAND, CHOOZ+atmospheric+K2K, and global data. Right: Allowed regions for $\sin^2\theta_{12}$ and $\sin^2\theta_{13}$ at 90%, 95%, 99%, and 3σ C.L. for solar neutrino data (solid contour lines), KamLAND (dashed contour lines), and solar+KamLAND data (coloured regions).

Label	L	$\langle E_\nu \rangle$	$t_{\rm run}$	channel
Conventional beam experiments:				
MINOS [17]	735 km	3 GeV	5 yr	$\nu_\mu \to \nu_\mu, \nu_e$
ICARUS [18]	732 km	17 GeV	5 yr	$\nu_\mu \to \nu_e, \nu_\mu, \nu_\tau$
OPERA [19]	732 km	17 GeV	5 yr	$\nu_\mu \to \nu_e, \nu_\mu, \nu_\tau$
Reactor experiments with near and far detectors:				
D-Chooz [20]	1.05 km	~ 4 MeV	3 yr	$\bar\nu_e \to \bar\nu_e$
Reactor-II [21]	1.70 km	~ 4 MeV	5 yr	$\bar\nu_e \to \bar\nu_e$
Off-axis super-beams:				
T2K [22]	295 km	0.76 GeV	5 yr	$\nu_\mu \to \nu_e, \nu_\mu$
NOνA [23]	812 km	2.22 GeV	5 yr	$\nu_\mu \to \nu_e, \nu_\mu$

Table 2: Summary of upcoming experiments.

solar and KamLAND experiments lead to a non-negligible contribution of these experiments to the global bound, especially for low values of Δm^2_{31} within the present allowed range [1]. From the left panel of Fig. 3 one deduces the following limits at 90% C.L. (3σ):

$$\sin^2\theta_{13} < \begin{cases} 0.029\,(0.067) & \text{CHOOZ+atm+K2K,} \\ 0.041\,(0.079) & \text{solar+KamLAND,} \\ 0.021\,(0.046) & \text{global data.} \end{cases} \qquad (2)$$

In the right panel of Fig. 3 we illustrate how the combination of solar and KamLAND data leads to a non-trivial bound on θ_{13}. The allowed regions in the plane of $\sin^2\theta_{12}$ and $\sin^2\theta_{13}$ show the complementarity of the two data sets, which follows from the very different conversion mechanisms: vacuum oscillations at a baseline of order 180 km for KamLAND, and adiabatic MSW conversion inside the sun for solar neutrinos. For a further discussion see the appendix of Ref. [2] or Ref. [16].

3 Prospects for the coming ten years

In this section I discuss the potential of long-baseline experiments, from which results are to be expected within the coming ten years. The first results will be obtained by the conventional beam experiments MINOS and the CNGS experiments ICARUS and OPERA. Subsequent information might be available from new reactor experiments. We take as examples D-Chooz as a first stage experiment, and a generic second-generation experiment labeled Reactor-II, which could be realized at sites in Brazil, China, Japan, Taiwan, or USA, see Ref. [21] for an overview. Towards the end of the anticipated time scale results from super-beam experiments T2K and NOνA could be available. The main characteristics of these experiments are summarized in Tab. 2. For the simulation the GLoBES software [24] is used. Technical details and experiment descriptions can be found in Refs. [3, 4, 25]. In the following I discuss the expected improvement on the leading atmospheric parameters, and the sensitivity to θ_{13}, the CP phase $\delta_{\rm CP}$ and the type of the neutrino mass hierarchy. A discussion of prospects to improve the determination of the leading solar parameters can be found in Ref. [26].

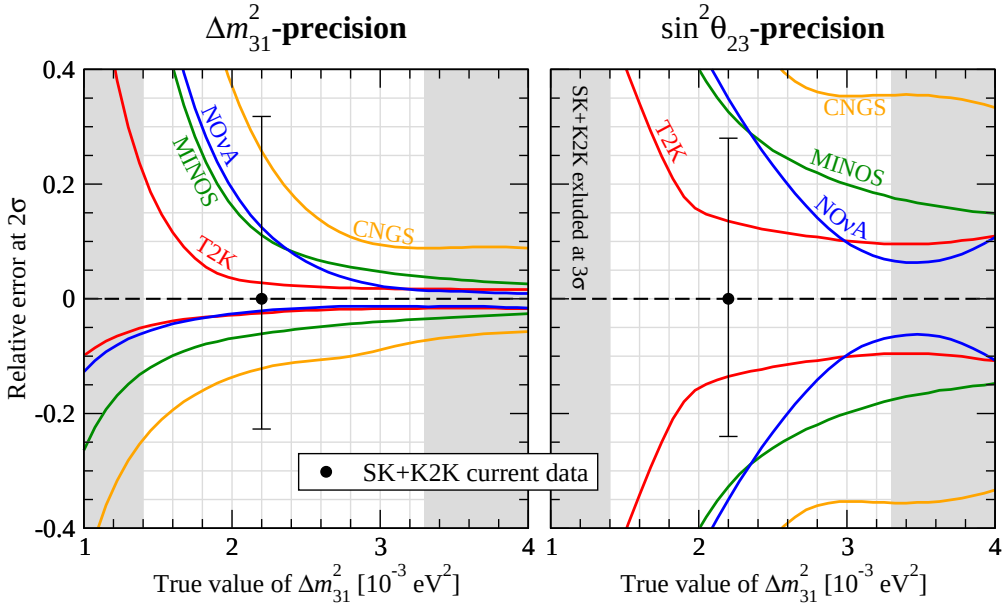

Figure 4: Prospective relative errors at 2σ on $|\Delta m^2_{31}|$ (left) and $\sin^2\theta_{23}$ (right) as a function of the true value of Δm^2_{31} and for the true value $\sin^2\theta_{23} = 0.5$. The dots with the error bars indicate the present accuracy at 2σ from atmospheric and K2K data. The gray shaded region is excluded at 3σ by present data.

The 'atmospheric parameters'. In Fig. 4 I show how the upcoming experiments will improve the accuracy on $|\Delta m^2_{31}|$ and $\sin^2\theta_{23}$. Already MINOS will decrease significantly the error on $|\Delta m^2_{31}|$. The non-trivial constraint on $|\Delta m^2_{31}|$ from the CNGS experiments results from the fact that in this analysis also the ν_μ disappearance channel is included for these experiments (see Ref. [4] for details). For not too small values of $|\Delta m^2_{31}|$ T2K will provide a determination of order 2% at 2σ, which corresponds roughly to an improvement of one order of magnitude with respect to the present error. However, from the right panel of Fig. 4 one observes that for most values of $|\Delta m^2_{31}|$ T2K will improve the accuracy on $\sin^2\theta_{23}$ only by a factor of 2 with respect to the present uncertainty. The main reason for this only modest improvement comes from the fact that disappearance experiments measure $\sin^2 2\theta_{23}$, and a small uncertainty on $\sin^2 2\theta_{23}$ translates into a relatively large error for $\sin^2\theta_{23}$, if θ_{23} is close to maximal mixing.

It is interesting to note that the lower bound on $|\Delta m^2_{31}|$ from NOνA is comparable to the one from T2K, however, the upper bound is significantly weaker because of a strong correlation between $|\Delta m^2_{31}|$ and $\sin^2\theta_{23}$. Also the $\sin^2\theta_{23}$ measurement of NOνA is affected by this correlation, which gets resolved only in the range $|\Delta m^2_{31}| \gtrsim 3 \times 10^{-3}$ eV^2. This correlation appears because the NOνA detector is optimized for electrons, whereas the atmospheric parameters are determined essentially by the ν_μ disappearance channel. Let me add that as in Ref. [4] we assume here a low-Z-calorimeter. Using the totally active scintillator detector (TASD) as proposed in Ref. [23] improves the performance of NOνA for the atmospheric parameters.

The limit on θ_{13}. Fig. 5 shows the limits which can be obtained on $\sin^2 2\theta_{13}$ by the experiments under consideration, if no signal for a finite θ_{13} is found. One observes that the conventional beams may improve the present limit roughly by factor of 2, D-Chooz by a factor of 4, and the super-beams by a factor of 6. An optimized reactor experiment could

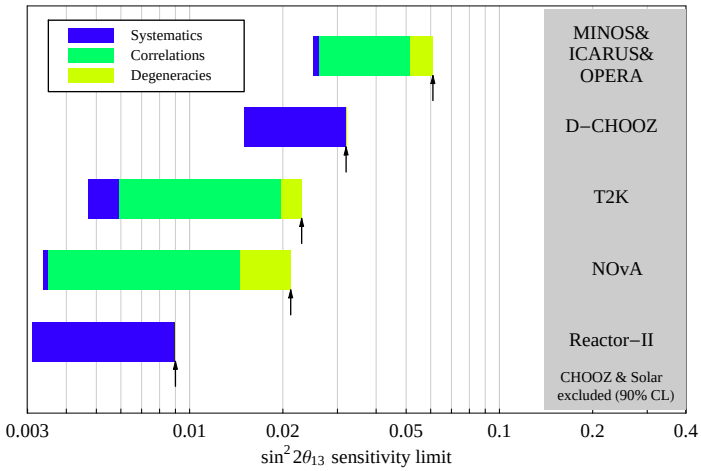

Figure 5: Sensitivity to $\sin^2 2\theta_{13}$ at 90% C.L. The left edges of the bars are obtained for the statistics limits only, whereas the right edges are obtained after successively switching on systematics, correlations, and degeneracies, *i.e.*, they correspond to the final sensitivity. The gray shaded region is excluded at 90% C.L. by present data. For the true values of the oscillation parameters, we use $\Delta m^2_{31} = +2.0 \times 10^{-3}\,\mathrm{eV}^2$, $\sin^2 2\theta_{23} = 1$, $\Delta m^2_{21} = 7.0 \times 10^{-5}\,\mathrm{eV}^2$, $\sin^2 2\theta_{12} = 0.8$.

improve the present bound by more than one order of magnitude, reaching a limit for $\sin^2 2\theta_{13}$ below 10^{-2} at 90% C.L. The limits shown in Fig. 5 depend on the true value of Δm^2_{31}; in general stronger limits can be reached for larger values of Δm^2_{31}.

The figure illustrates that the $\sin^2 2\theta_{13}$ limits from $\nu_\mu \to \nu_e$ appearance beam experiments are strongly affected by correlations, mainly between $\sin^2 2\theta_{13}$ and δ_{CP}. The bars labeled 'Degeneracies' originate from the fact that the hierarchy cannot be determined, and the sensitivity is quoted for the hierarchy which gives the worse limit (see the appendix of Ref. [4] for a detailed discussion of the sensitivity limit). Clearly, the $\sin^2 2\theta_{13}$ limit from reactor experiments is completely free from correlations and degeneracies [3,27], since the $\bar{\nu}_e$ survival probability does not depend on δ_{CP} and θ_{23}, and the dependence on the solar parameters is negligibly small. These experiments are dominated by systematical uncertainties, related mainly to the comparison of the near and far detectors. A possibility to reduce significantly the impact of these uncertainties has been presented in Ref. [28].

Possibilities for large θ_{13}. Finally I discuss the potential of the experiments of Tab. 2 if θ_{13} is not too far from the present upper bound. In Fig. 6 the allowed regions in the $\sin^2 2\theta_{13}$-δ_{CP} plane are shown assuming a true value of $\sin^2 2\theta_{13} = 0.1$. For the super-beam experiments T2K and NOνA one observes the strong correlation between $\sin^2 2\theta_{13}$ and δ_{CP}, which introduces a large uncertainty in $\sin^2 2\theta_{13}$ but does not permit to draw any conclusions on δ_{CP}. In contrast, the reactor experiment provides an accurate measurement of $\sin^2 2\theta_{13}$ with an accuracy at the level of 10% at 90% C.L. None of the experiments on its own can identify the mass hierarchy. As indicated in the figure, the best fit point of the wrong hierarchy is as good as the true best fit point. However, from the combination of T2K+NOνA+Reactor-II the wrong hierarchy can be disfavoured with $\Delta\chi^2 = 3.1$, which corresponds roughly to the 90% C.L. The crucial element for the mass hierarchy determination is the long baseline of 812 km for NOνA, leading to matter effects which allow to distinguish between normal and inverted hierarchy. Let me add, that the hierarchy sensitivity strongly depends on the true value of δ_{CP}; typically it is optimal for $\delta_{\mathrm{CP}} \simeq -90°$, and worst for $\delta_{\mathrm{CP}} \simeq 90°$ [4].

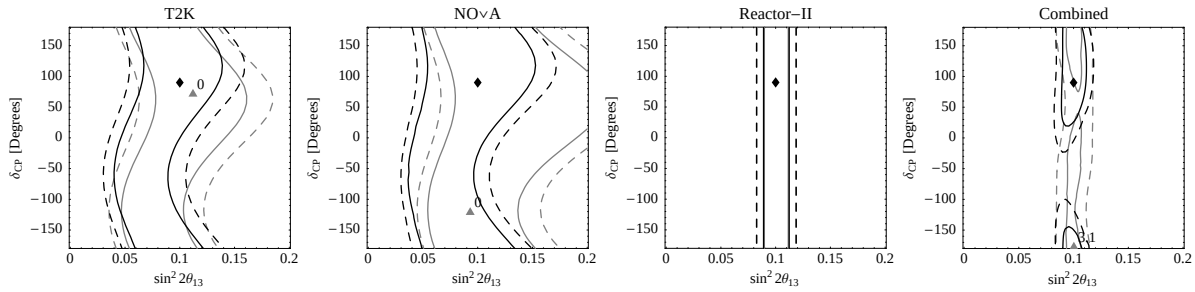

Figure 6: The 90% C.L. (solid) and 3σ (dashed) allowed regions (2 d.o.f.) in the $\sin^2 2\theta_{13}$-$\delta_{\rm CP}$ plane for the true values $\sin^2 2\theta_{13} = 0.1$ and $\delta_{\rm CP} = 90^\circ$. The black curves refer to the allowed regions for the normal mass hierarchy (assumed to be the true hierarchy), whereas the gray curves refer to the $\mathrm{sgn}(\Delta m^2_{31})$-degenerate solution (inverted hierarchy), where the projections of the minima onto the $\sin^2 2\theta_{13}$-$\delta_{\rm CP}$ plane are shown as diamonds (normal hierarchy) and triangles (inverted hierarchy). For the latter, the $\Delta\chi^2$-value with respect to the best-fit point is also given.

As visible from Fig. 6 no information can be obtained on CP violation, *i.e.*, at least one of the CP-conserving values $\delta_{\rm CP} = 0, 180^\circ$ is contained within the 90% C.L. region, even though the assumed true value $\delta_{\rm CP} = 90^\circ$ corresponds to maximal CP violation. The reason is that no anti-neutrino data is included in this analysis, since due to the low cross sections it seems unlikely that significant anti-neutrino data will be available within the anticipated time scale. Note however, that from the combined analysis some values of $\delta_{\rm CP}$ can be excluded for a given mass hierarchy.

4 Conclusions

I have reviewed the present status of neutrino oscillations from world neutrino oscillation data, including solar, atmospheric, reactor and accelerator experiments. The results of a global analysis within the three-flavour framework have been presented, and in particular, the bound on θ_{13}, which emerges from the interplay of various data sets has been discussed. Furthermore, a prospect on where we could stand in neutrino oscillations in ten years from now has been given. Based on a simulation of upcoming long-baseline accelerator and reactor experiments the improvements on the leading atmospheric parameters, as well as the sensitivity to θ_{13}, $\delta_{\rm CP}$ and the neutrino mass hierarchy have been discussed.

Acknowledgments

I thank the organizers for the very pleasant and interesting conference. The results presented here have been obtained in collaboration with P. Huber, M. Lindner, M. Maltoni, M. Rolinec, M.A. Tórtola, J.W.F. Valle and W. Winter. T.S. is supported by a "Marie Curie Intra-European Fellowship within the 6th European Community Framework Program."

References

[1] M. Maltoni, T. Schwetz, M.A. Tórtola and J.W.F. Valle, Phys. Rev. D **68**, 113010 (2003) [hep-ph/0309130].

[2] M. Maltoni, T. Schwetz, M.A. Tórtola and J.W.F. Valle, New J. Phys. **6** (2004) 122 [hep-ph/0405172].

[3] P. Huber, M. Lindner, T. Schwetz and W. Winter, Nucl. Phys. B **665**, 487 (2003) [hep-ph/0303232].

[4] P. Huber, M. Lindner, M. Rolinec, T. Schwetz and W. Winter, Phys. Rev. D **70**, 073014 (2004) [hep-ph/0403068].

[5] B. T. Cleveland *et al.*, Astrophys. J. **496** (1998) 505; J.N. Abdurashitov *et al.* (SAGE), J. Exp. Theor. Phys. **95** (2002) 181 [astro-ph/0204245]; T. Kirsten *et al.* (GALLEX and GNO), Nucl. Phys. B (Proc. Suppl.) **118** (2003) 33; C. Cattadori, Talk given at Neutrino04, June 14-19, 2004, Paris, France; S. Fukuda *et al.* (Super-K), Phys. Lett. **B539** (2002) 179.

[6] Q.R. Ahmad *et al.* (SNO), Phys. Rev. Lett. **89**, 011302 (2002) [nucl-ex/0204009].

[7] B. Aharmim *et al.* (SNO), nucl-ex/0502021.

[8] Super-K Coll., Y. Fukuda *et al.*, Phys. Rev. Lett. **81** (1998) 1562 [hep-ex/9807003]; Y. Ashie *et al.*, Phys. Rev. D **71** (2005) 112005 [hep-ex/0501064].

[9] T. Araki *et al.* (KamLAND), Phys. Rev. Lett. **94**, 081801 (2005) [hep-ex/0406035].

[10] M. Apollonio *et al.* (CHOOZ), Eur. Phys. J. C **27**, 331 (2003) [hep-ex/0301017].

[11] E. Aliu *et al.* (K2K), Phys. Rev. Lett. **94**, 081802 (2005) [hep-ex/0411038].

[12] M.C. Gonzalez-Garcia, M. Maltoni and A.Y. Smirnov, Phys. Rev. D **70** (2004) 093005 [hep-ph/0408170].

[13] G. L. Fogli, E. Lisi, A. Marrone and A. Palazzo, hep-ph/0506083.

[14] Talk by T. Kajita at NuFact05, June 21–26, Frascati, Italy, http://www.lnf.infn.it/conference/nufact05/talks2/WG1/Kajita_WG1.ppt

[15] P. Huber and T. Schwetz, Phys. Rev. D **70** (2004) 053011 [hep-ph/0407026].

[16] S. Goswami and A.Y. Smirnov, Phys. Rev. D **72**, 053011 (2005) [hep-ph/0411359].

[17] E. Ables *et al.* (MINOS) FERMILAB-PROPOSAL-P-875.

[18] P. Aprili *et al.* (ICARUS) CERN-SPSC-2002-027.

[19] D. Duchesneau (OPERA), eConf **C0209101**, TH09 (2002) [hep-ex/0209082].

[20] F. Ardellier *et al.*, Letter of intent for Double-CHOOZ: A search for the mixing angle θ_{13}, hep-ex/0405032.

[21] K. Anderson *et al.*, White paper report on using nuclear reactors to search for a value of θ_{13}, hep-ex/0402041.

[22] Y. Itow *et al.*, The JHF-Kamioka neutrino project, hep-ex/0106019.

[23] D.S. Ayres *et al.*, NOvA proposal to build a 30-kiloton off-axis detector to study neutrino oscillations in the Fermilab NuMI beamline, hep-ex/0503053.

[24] P. Huber, M. Lindner and W. Winter, Comput. Phys. Commun. **167**, 195 (2005) [hep-ph/0407333]; GLoBES webpage: http://www.ph.tum.de/∼globes/.

[25] P. Huber, M. Lindner and W. Winter, Nucl. Phys. B **654** (2003) 3 [hep-ph/0211300]; Nucl. Phys. B **645** (2002) 3 [hep-ph/0204352].

[26] J.N. Bahcall and C. Peña-Garay, JHEP **0311** (2003) 004 [hep-ph/0305159]; A. Bandyopadhyay, S. Choubey, S. Goswami and S.T. Petcov, Phys. Rev. D **72** (2005) 033013 [hep-ph/0410283].

[27] H. Minakata, H. Sugiyama, O. Yasuda, K. Inoue and F. Suekane, Phys. Rev. D **68** (2003) 033017, Erratum-ibid. D **70** (2004) 059901 [hep-ph/0211111].

[28] P. Huber, M. Lindner and T. Schwetz, JHEP **0502** (2005) 029 [hep-ph/0411166].